Hot-spots generation, exaggerated grain growth and mechanical performance of silicon carbide bulks consolidated by flash spark plasma sintering

Dmytro Demirskyi (a) and Oleg Vasylkiv (a,b).

(a) Nanyang Technological University, 50 Nanyang Avenue, 639798 Singapore

(b) National Institute for Materials Science, 1-2-1 Sengen, Tsukuba, Ibaraki 305-0047, Japan

Corresponding Authors:

Dmytro Demirskyi, phone: +65-93415641, e-mail: dmytro.demirskyi@ntu.edu.sg,

Oleg Vasylkiv, phone: +81-8041444747, e-mail: oleg.vasylkiv@nims.go.jp.

Abstract

Flash Spark Plasma Sintering (FSPS) that combines flash sintering and electric field assisted sintering was used to densify SiC ceramics. FSPS was compared with 'conventional' SPS which used a moderate 100 °C·min^{-1} heating rates. Dense SiC specimens were obtained despite being at temperature of 1850–2050 °C for few seconds. FSPS lead to generation of hot-spots and thus caused localized exaggerated grain-growth. This allows producing silicon carbide ceramics with bimodal grain size distribution. Analysis of microstructure and strength of FSPS specimens allowed proposing several optimization routes of the FSPS process.

Keywords: spark plasma sintering; flash sintering; carbon diffusion; silicon carbide; strength.

1. Introduction

There is an unstoppable trend for quicker fabrication of ceramic materials. Within last few decades methods like microwave sintering or spark plasma sintering (SPS) showed that

conventionally hard to sinter materials can be heat-up to sintering temperature using heating rates exceeding 100 °C·min^{-1} and consolidated within minutes [1–6]. Flash sintering (FS) approach squeezes processing time to seconds at relatively low-temperatures [7]. Originally, FS experiments were focused mainly on consolidation of various oxide ceramics and had a limitation of size and share [7]. Recent studies show that by using modification to original FS techniques non-oxide compounds such as SiC, ZrB_2 or B_4C ceramics may be consolidated using 'flash' regime [8–12]. Grasso et al. [11], in particular, showed that consolidation of large size specimens of SiC (60 mm in diameter) can be completed within minutes using the flash SPS (FSPS) method. Due to abandoning of graphite mold-punches set-up, heating during FSPS is mainly controlled by ceramic sample properties. Furthermore, FSPS approach showed that temperature distribution inside flashed specimens can be lead to creation of hot-spots. Using FSPS approach Vasylkiv at al. successfully reported consolidation of the 3YSZ ceramics with size of 20 mm in diameter [13]. Taking into account a possibility of producing relatively large size specimens by both works [11,13], it is natural to seek whether the consolidation by FSPS of such advanced ceramics as SiC [14–17] may lead to improvement of mechanical properties.

Hence, the aim of this study was to consolidate commercially available SiC powder by the FSPS method targeting large size specimens. Secondly, to explore the difference between flash SPS and regular SPS while using identical hardware. Finally, to verify whether FSPS can be utilized to consolidate bulk SiC specimens and lead to increase in mechanical properties such as flexural strength at room temperature and at 1600 °C.

2. Materials and Methods

Commercially available beta silicon carbide (β-SiC UF, Ibiden Co., Gifu, Japan) and amorphous boron (aB, 97%, Wako Pure Chemical Industries, Ltd., Osaka, Japan) [18] powders were used as the starting materials (**Fig. 1**). Silicon carbide with 1 wt.% aB mixture was homogenized using wet mixing in alcohol, followed by drying at about 100 °C. The resultant powders were screened through a 60, 400 and 1250 mesh screens.

The homogenized powder mixture was loaded into a graphite die with an inner diameter of 30 and 50 mm and subjected to SPS. The outer surface of the die was wrapped in 5-mm-thick graphite felt to homogenize the temperature distribution and reduce heat loss by radiation. The mold system containing the powder mixture was placed in an SPS furnace ('Dr. Sinter' SPS Syntex 1050, Japan) [11].

A two stage consolidation process was used to produce FSPS and SPS specimens. First, specimens with diameter of 30 or 50 mm and high of 5–7 mm were prepared by the preliminary SPS consolidation at 1200 °C. The samples were heated under vacuum to 1200 °C at 100 °C·min^{-1} under axial pressure of 60 MPa. After 20 minutes of dwell at this intermediate step, samples for the FSPS were cooled down to room temperature at a rate of 100 °C·min^{-1} (**Fig. 2 (a)**). The specimens were evacuated from the graphite die and were subjected to the mold-free [11–13] FSPS consolidation. This step consisted of wrapping the pre-consolidated SiC specimens with additional graphite foils and putting them into set-up in depth described in [13].

The temperature during FSPS experiments was probed by the side pyrometer focused on the side of the graphite felt using an emissivity of 0.90. In FSPS experiments, a constant uniaxial pressure of 20 MPa was applied. The samples were discharged under a peak power of about for about 5–20 seconds (**Fig. 3**). The power was switched off after selected discharge time, and specimens

were allowed to cool to room temperature under unchanged pressure conditions. FSPS experiments were performed in argon gas with a flow rate of 2 $L \cdot min^{-1}$.

For the reference, the samples were also sintered using a conventional SPS configuration. For these studies, SPS was continued after an intermediate step at 1200 °C. Thus, after the 20 minute dwell at 1200 °C, the SPS chamber was backfilled with argon, and pre-consolidated SiC specimens were heated up to 1900 °C at a rate of 100 $°C \cdot min^{-1}$ and were held for 15 minutes (**Fig. 2(b)**). The pressure of 60 MPa was maintained during consolidation and cooling stages. Each specimen was gradually cooled to 600 °C at a rate of 100 $°C \cdot min^{-1}$ and then naturally to room temperature in the furnace. Argon gas with a flow rate of 2 $L \cdot min^{-1}$ was used.

The sintered specimens were ground with diamond disks with a particle size of up to 0.5 μm. Then, the density of the samples was measured by the Archimedes method using ethanol as a medium in accordance with ASTM B 963–08.

The three-point flexural strength was determined using rectangular bars (2 × 2.5 × 20 mm) cut from specimens with a diameter of 30 and 50 mm using electric discharge machining. Their lateral surfaces were ground and polished using diamond pastes.

The flexural strength tests were conducted at room temperature and at 1600 °C in argon using a Shimadzu AG-X plus system (Shimadzu, Japan). The loading speed was 0.5 $mm \cdot min^{-1}$. Twelve bars were tested at room temperature, and five specimens at 1600 °C. For the flexural strength tests at 1600 °C, the following heating schedule was used: from room temperature to 200 °C in 10 min and from 200 °C to the testing temperature at a rate of 18 $°C \cdot min^{-1}$ [19]. A dwell time of 5 min was employed before the flexural test at the testing temperature. After testing, cooling from the testing temperature to room temperature was performed at a rate of 20 $°C \cdot min^{-1}$.

Microstructural observations and analyses were carried out on the fracture surfaces using scanning electron microscopes (SEM) SU 8000 cold-emission FE-SEM Hitachi and JEOL 6500F equipped with energy dispersive spectroscopy (EDS) detectors. Observations were made on fractured surfaces after bending tests.

3. Results and Discussion

Figure 3 shows analysis of raw data obtained for SiC tile #1f consolidated using flash spark plasma sintering method. Fig. 3 (a) shows the output of the Sumitomo SPS machine recorded during FSPS. Flash consolidation does not start from the moment when electrical power if turned on: some incubation time is required, i.e. preheating stage [11,13], for sample to become conductive. This is followed by the 'flash' heating of the specimens: temperature increases from 900 °C to 1900 °C within 20 seconds. Furthermore, SiC tile does not shrink instantly with electrical current passing through as some increase in volume is observed on the incubation stage. Only at 1370±25 °C (**Figs. 3 (a, b)**) shrinkage becomes significant and a consolidation of silicon carbide sample by FS begins.

Figure 3 (a) shows that FSPS of silicon carbide specimens usually lasts at most 3 minutes. In the present study, we controlled temperature of FSPS and discharge time by controlling the maximum power of the SPS machine. Sample #1f reached a temperature of 1935±7 °C that was kept for 21 s, using a current of 3610 A and voltage of 6.10 V. This yields a power of 22 kW, which is twice larger than that used by Grasso et al. in [11] for specimens with diameter of 20 mm. The cooling stage requires additional attention: an increase in voltage during switch-off procedure caused a rapid change in shrinkage (**Fig. 3 (c)**). A non-linear shrinkage behavior with negative and positive shrinkage 'humps' was observed during a quasi-liner cooling after FSPS.

Density measurements suggested that densities of consolidated ceramics specimens were over 92 % of theoretical density. For ceramics produced by a two-stage SPS a mean grain size of SiC grains was evaluated as 3.3±0.7 μm, some equiaxed grains with size up to 10 μm were also present (**Fig. 4**). FSPS promoted a clear bimodal grain size distribution inside consolidated specimens: the size of the large grains depended largely on the FSPS conditions such as consolidation temperature and discharge time (**Table 1**).

As noted above, FSPS process lasts up to 3 minutes which include heating and cooling stages. These are unnatural processing conditions even for SiC ceramics with excellent thermal shock resistance properties [17]. Hence it is unsurprising that only 4 of 9 specimens attempted were free of macroscopic cracks and thus were passed for cutting and evaluation of the flexural strength. A spontaneous internal microcracking frequently occurs in polycrystalline ceramics during cooling from the densification temperature, as a result of anisotropic thermal expansion coefficients or grain-growth [20]. Another factor to consider is fast decrease in temperature which is associated with end of electric current flow at the end of FSPS. This causes a thermal shock due to the sudden decrease of the temperature to 900 °C. Stresses are generated by temperature differences between the interior and surface of a specimen, the maximum stress is the tensile stress on the surface and the center is in compression [21].

Interestingly, in the present study we found out that increasing of the discharge time over 15 s increases chances of obtaining of crack-free specimens. This observation is not fully understood at this moment, but it may be connected with temperature homogenization inside the SiC specimens during extended discharge time. Unfortunately, an increase in discharge time increases time for the grain-growth process. Hence, it is suggested that further optimization of the dwell or cooling stages should be performed.

Fractographic analysis of the specimen after flexural tests suggests that breakage occurred mainly in intergranular manner (**Figs. 4** and **5**). This is typical fracture mode for silicon carbide ceramics [22]. The presence of small sized boron carbide grains was obvious for SPS specimens, as well as presence of fine carbon inclusions. Surprisingly, the increased number of carbon inclusions was observed for FSPS specimens. Few boron carbide grains were detected during fractographic analysis (see inset EDS mapping of boron for #e6 in **Fig. 5(c)**), their size was smaller than that observed for SPSed specimen (**Fig. 4**). Increased number of carbon inclusion and their presence inside equiaxed SiC grains (see **Fig. 5 (a)**) is currently unclear. It was believed that by using mold-free configuration and ultra-short consolidation time using FSPS configuration, carbon diffusion will be a minor issue [19].

It is known that for β-SiC the presence of an excess in boron may result in the exaggerated grain growth [23–25], hence only 1 wt.% of the amorphous boron powder in the present study, and the main purpose was to decrease a number of carbon inclusions. A controlled number of carbon additions had a positive effect on densification of SiC by manipulating SiO_2/SiC interaction at lower temperatures [25]. The mechanism of boron's contribution to sintering is due to its lowering of the grain boundary to surface energy ratio, by segregating to the grain boundaries [24]. Thus the grain growth is driven by surface energy stored in fine grains, which firstly causes rapid growth of β-SiC powder grains, some of them becoming large plate- or rod shape.

In the case of a two-step SPS, boron interacted with residual carbon, hence small boron carbide grains were formed (**Fig. 4 (c)**), and some carbon inclusions were still present. In the FSPS case, boron carbide grains had smaller size than that obtained by two-step SPS. This is due to a limited time for reaction and growth of the newly formed B_4C phase during FSPS. Therefore, the increased number of carbon inclusions observed as black phase in **Fig. 5 (a)** may be initiated by

the generation of the hot-spots inside specimen, which may act as a factor for promoting carbon diffusion. Such quick carbon diffusion was previously reported during spark plasma sintering at comparatively lower temperatures [26] and is believed to be a characteristic feature of the SPS method. One can expect that, different results may be achieved by adding boron carbide instead of boron [11].

Other possible solution which proved it efficiency for SPS of boron suboxide ceramics is by blocking carbon diffusion using Ta foil [19]. However, in the latter case, tantalum foil may act as an additional indirect heater, which changes flashing behavior of pre-consolidated SiC specimens.

The example of such processing can be seen in **Fig. 6**. Firstly, the incubation time becomes shorter because the Ta (or TaC during the later stages of FSPS) has higher conductivity than SiC and thus acts as a an additional heater during FSPS. Within twenty seconds after electric current is turned on, specimen reaches temperature of 1153 °C. This is followed by a rapid increase in temperature up to 1973±20 °C, where sample was discharged for 15 s. A total power used at dwell was 17.4 kW, which is less than estimated for #1f. This may be connected with direct current flow through the Ta foil. It is worth mentioning that after FSPS experiment, the tantalum foil had a yellow color, which is typical for tantalum carbide. Ta foil reacted with additional graphite felt that we use in a typical FSPS experiment to preheat the sample. This underlines that carbon diffusion from the SPS die-punches set-up or even graphite foil is well underestimated if the consolidation is performed at elevated temperatures [19,26]. Nevertheless our trial on FSPS with tantalum foil resulted in a crack-free specimen, which was passed for flexural strength measurements. **Figure 7** shows that tantalum foil affected the consolidation conditions during FSPS: a mixture of small size (10–20 μm in length) and large size (40–100 μm in length)

nonequiaxial silicon carbide grains was observed. Most noticeably, this specimen had fewer amount of carbon inclusions than that for FSPS specimens without Ta foil (compare with **Fig. 5 (a)**).

To compare the mechanical performance of bulk crack-free specimens prepared by SPS in conventional and flash regimes, the flexural strength at room temperature and at 1600 °C been evaluated. The strength of the SPSed SiC specimens was about 450±10 MPa. It did not degraded at 1600 °C which is consistent with earlier findings of Tanaka et al. for Al-doped β-SiC [23, 27]. FSPSed SiC specimens showed strength degradation when testing temperature increased to 1600 °C (see **Table 1**). This may be attributed to a number of parameters such as (i) different density [23], (ii) structural inhomogeneity i.e. presence of clusters with the exaggerated grain growth, (iii) insufficient time to develop 'strong' grain-boundary framework [28] or (iv) presence of carbon inclusions. Most likely, the combination of all above-mentioned factors affects strength behavior of FSPSed SiC specimens. The exception was #Tae6 specimen which showed comparatively low strength at room-temperature (391±17 MPa), and showed no degradation in strength at 1600 °C (387±15 MPa). It appears that, in this case different consolidation conditions resulted in fewer hot-spots and thus different size of clusters with exaggerated grain growth.

Properties such as toughness benefit from plate-like grains that result from β to α transformation of SiC. Padture at al. [15,16] showed that the layer-by-layer transformation of silicon carbide which leads to a bimodal grain structure, can be utilized to further enhancement in properties. In this respect, FSPS of SiC with controlled distribution of the hot-zones (and thus large-size grains) inside the flashed specimen should become a priority for further research.

We consider this research as a pilot attempt to consolidate large-size tiles using FSPS method and Sumitomo SPS hardware. In order to fully understand the observed results, tailoring of the FSPS parameters such as discharge time or cooling conditions are suggested as next steps in upcoming research. Taking into account a positive and unexpected effect of tantalum foil during flash spark plasma sintering of SiC, one may expect that silicon carbide ceramics with good toughness at room and elevated temperatures are within reach for this rapidly developing consolidation method.

Concluding remarks

The experiments with flash spark plasma sintering of silicon carbide using mold-free SPS set-up give possibility to produce dense specimens with diameter of 30 or 50 mm. SiC bulks prepared by FSPS showed densities exceeding 91% and had a bimodal grain size distribution with >20 μm size equiaxed grains. FSPS specimens exhibited strength of 400±20 MPa at room temperature. Highest strength for FSPSed SiC at 1600 °C was 387±15 MPa for the specimen consolidated using a tantalum foil. Ta foil changes heating behavior of the silicon carbide specimen and suppresses to some point carbon diffusion during FSPS. The SiC ceramics prepared by a conventional two-step SPS showed a stable strength within 450±20 MPa at room temperature and at 1600 °C. Nevertheless, the FSPS offers a significant decrease in processing time compared to SPS, i.e. 3 min vs 33 min. Further optimization of processing parameters to control grain-boundary framework development is vital in order to achieve high-performance ceramics using abnormally short processing time.

Acknowledgments

We thank to Dr. Toshiyuki Nishimura (NIMS) for the use of strength measurements apparatus. We also express our gratitude to Hidehiko Tanaka (NIMS) for his advice in the interpreting of fracture behavior of SiC specimens.

References

[1] T. Gerdes, M. Willert-Porada, "Microwave sintering of metal–ceramic and ceramic–ceramic composites," *Mater. Res. Soc. Symp. Proc.*, **347** (1994) 531–537.

[2] O. Vasylkiv, D. Demirskyi, Y. Sakka, A. Ragulya, H. Borodianska, "Densification Kinetics of Nanocrystalline Zirconia Powder Using Microwave and Spark Plasma Sintering—A Comparative Study," *J. Nanosci. Nanotechnol.*, **12** (2012) 4577–4582.

[3] D. Demirskyi, O. Vasylkiv, "Microstructure and mechanical properties of boron suboxide ceramics prepared by pressureless microwave sintering," *Ceram. Int.*, **42** (2016) 14282–14286.

[4] O. Vasylkiv, D. Demirskyi, P. Badica, T. Nishimura, A.I.Y. Tok, Y. Sakka, H. Borodianska, "Room and high temperature flexural failure of spark plasma sintered boron carbide," *Ceram. Int.*, **42** (2016) 7001–7013.

[5] D. Demirskyi, Y. Sakka, O. Vasylkiv, "High-temperature reactive spark plasma consolidation of TiB2–NbC ceramic composites," *Ceram. Int.*, **41** (2015) 10828–10834.

[6] D. Demirskyi, T. Nishimura, Y. Sakka, O. Vasylkiv, "High-strength TiB2–TaC ceramic composites prepared using reactive spark plasma consolidation," *Ceram. Int.*, **42** (2016) 1298–1306.

[7] M. Cologna, B. Rashkova, R. Raj, "Flash sintering of nanograin zirconia in <5 s at 850 C," *J. Am. Ceram. Soc.*, **93** (2010) 3556−3559.

[8] E. Zapata-Solvas, S. Bonilla, P.R. Wilshaw, R.I. Todd, *J. Eur. Ceram. Soc.*, "Preliminary investigation of flash sintering of SiC," **33** (2013) 2811−2816.

[9] B. Niu, F. Zhang, J. Zhang, W. Ji, W. Wang, Z. Fu, "Ultra-fast densification of boron carbide by flash spark plasma sintering," *Scr. Mater.*, **116** (2016) 127–130.

[10] S. Grasso, T. Saunders, H. Porwal, O. Cedillos-Barraza, D. Jayaseelan, W.E. Lee, M. Reece, "Flash spark plasma sintering (FSPS) of pure ZrB2," *J. Am. Ceram. Soc.*, **97** (2014) 2405–2408.

[11] S. Grasso, T. Saunders, H. Porwal, B. Milsom, A. Tudball, M. Reece, "Flash Spark Plasma Sintering (FSPS) of α and β SiC," *J. Am. Ceram. Soc.*, **99** (2016) 1534–1543.

[12] S. Grasso, E.-Y. Kim, T. Saunders, M. Yu, A. Tudball, S.-H. Choi, M. Reece, "Ultra-Rapid Crystal Growth of Textured SiC Using Flash Spark Plasma Sintering Route," *Cryst. Growth Des.*, **16** (2016) 2317–2321.

[13] O.Vasylkiv, H. Borodianska, Y. Sakka, D. Demirskyi, "Flash spark plasma sintering of ultrafine yttria-stabilized zirconia ceramics," *Scr. Mater.*, **121** (2016) 32–36.

[14] J.E. Lane, C.H. Carter Jr., R.F. Davis, "Kinetics and Mechanisms of High-Temperature Creep in Silicon Carbide: III, Sintered α-Silicon Carbide," *J. Am. Ceram. Soc.*, **71** (1988) 281–295.

[15] N.P. Padture, "In Situ-Toughened Silicon Carbide," *J. Am. Ceram. Soc.* **77** (1994) 519–523.

[16] N.P. Padture, D.C. Pender, S. Wuttiphan, B.R. Lawn, "In Situ Processing of Silicon Carbide Layer Structures," *J. Am. Ceram. Soc.*, **78** (1995) 3160–3162.

[17] G. G. Gnesin, Oxygen-Free Ceramic Materials, Tekhnika, Kiev (1987) [in Russian].

[18] I. Solodkyi, D. Demirskyi, Y. Sakka, O. Vasylkiv, "Synthesis of Multilayered Star-Shaped B6O Particles Using the Seed-Mediated Growth Method," *J. Am. Ceram. Soc.*, **98** (2015) 3635–3638.

[19] D. Demirskyi, I. Solodkyi, Y. Sakka, O. Vasylkiv, "High-Temperature Strength of Boron Suboxide Ceramic Consolidated by Spark Plasma Sintering," *J. Am. Ceram. Soc.,* (doi:10.1111/jace.14308).

[20] H.R. Baumgartner, R.A. Steiger, "Sintering and properties of titanium diboride made from powder synthesized in a plasma-arc heater," *J. Am. Ceram. Soc.*, **67** (1984) 207–212.

[21] W.D. Kingery, "Factors Affecting Thermal Stress Resistance of Ceramic Materials," *J. Am. Ceram. Soc.*, **38** (1955) 3–15.

[22] T.D. Gulden, *J. Am. Ceram. Soc.*, "Mechanical Properties of Polycrystalline β-Sic," **52** (1969) 585–590.

[23] H. Tanaka, "Sintering of silicon carbide," in Silicon Carbide Ceramics, ed. S. Somiya and Y. Inomata. Elsevier Applied Science, London, 1991, pp. 213–238.

[24] S. Prochazka, "The Role of Boron and Carbon in the Sintering of Silicon Carbide," in Special Ceramics, Vol. 6. Ed. P. Popper. Institute of Ceramics, Stoke-on-Trent, U.K., 1975, pp. 171–181.

[25] W.J. Clegg, "Role of Carbon in the Sintering of Boron-Doped Silicon Carbide," *J. Am. Ceram. Soc.*, **83** (2000) 1039–1043.

[26] D. Demirskyi, H. Borodianska, D. Agrawal, A. Ragulya, Y. Sakka, O. Vasylkiv, "Peculiarities of the neck growth process during initial stage of spark-plasma, microwave and conventional sintering of WC spheres," *J. Alloys Compd.*, **523** (2012) 1–10.

[27] H Tanaka, Y Inomata, K Hara, H Hasegawa, "Normal Sintering of Al-Doped β-SiC," *J. Mat. Sci. Lett.*, **4** (1985) 315–317.

[28] O. Vasylkiv, H. Borodianska, P. Badica, S. Grasso, Y. Sakka, A. Tok, L. Su, M. Bosman, and J. Ma, "High Hardness BaCb-(BxOy/BN) Composites with 3D Mesh-Like Fine Grain-

Boundary Structure by Reactive Spark Plasma Sintering," *J. Nanosci. Nanotechnol.*, **12** (2012) 959–965.

Tables

Table 1 Physical and mechanical properties of SiC ceramics consolidated by SPS in the flash and conventional regimes.

Designation, diameter of die, mm	Tfsps,°C / discharge time in s	Density, g/cm^3 ǂ	Fractional density, %	Average grain size, μm	Presence of cracks	Flexural strength, MPa	
						RT	1600°C
0s / 30	1833±7 / 6	2.932	91.33	8–20	Macroscopic	-	-
1f / 30	1935±7/ 21	3.056	95.20	10±4.2 40–60*	-	422±23	287±32
2e / 30	1951±6 / 10	3.042	94.76	13–70	Macroscopic Microscopic	-	-
4e / 50	2018±11 / 3	3.155	98.28	8–50	Macroscopic Microscopic	-	-
6e / 50	1967±12/ 18	3.120	97.19	11±3.2 60–80*	Microscopic!	387±33	173±26
21 / 50	1951±5 / 10	3.092	96.32	8–80	Macroscopic Microscopic	-	-
88 / 50	2053±7 / 10	3.133	97.60	12–90	Macroscopic	-	-
26 / 50	1908±11 / 18	3.166	98.62	12.3±4.5 20–30*	-	412±13	310±44
Tae6 / 30	1973±20/ 15	3.109	96.85	6–18 40–100*	Microscopic!	391±17	387±15
CSPS7, 30	-	3.187	99.28	3.3±0.7 10*	-	455±13	461±12

Notes:

* Size of large equiaxed grains

ǂ Density for crack-free specimens was determined on the polished surfaces free of graphite foil. Density for cracked specimens was averaged for at least 4 four different pieces.

! Observed after flexural strength tests at room temperature or at 1600 °C.

Figure captions

Fig. 1. SEM images of initial β-SiC (a,b) and amorphous boron (c,d) powders.

Fig. 2. Mechanical load and temperature regimes used during the spark plasma sintering of silicon carbide ceramics. (a) shows a pre-consolidation step used for preparing specimens for FSPS, (b) shows a two-step schedule used for the SPS.

Fig. 3. Spark plasma sintering details of silicon carbide using FSPS method. (a) illustrates SPS output data recorder during consolidation of the specimen #1f by flash spark plasma sintering method. Dotted lines correspond to the temperature at which shrinkage becomes significant. This temperature (1370±25 °C) was identical for all specimens consolidated within the present study. (b) shows the effect of temperature on shrinkage during heating and cooling stages. (c) and (d) show the SPS output for the dashed area in (a): rapid increase in shrinkage after power was shut-down may be connected to the rapid increase in voltage.

Fig. 4. Typical fracture surfaces of bulk SiC specimens #CSPS7 consolidated by two-step SPS schedule (**Fig. 2 (b)**) after flexural strength tests at room-temperature (a, b) and at 1600 °C (c,d).

Fig. 5. Typical fracture surfaces of bulk SiC specimens consolidated flash SPS after flexural strength tests at 1600 °C: (a, b) – #1f, (c,d) – #e6, and (e,f) – #26 (see **Table 1**). Mind a different magnification in case of (c,d) was used to show the exaggerated grain growth which is believed to be caused by generation of hot-spots during FSPS. Inset in (a) shows typical carbon inclusion entrapped in SiC grains. Inset in (c) shows boron mapping for the (d).

Fig. 6. SPS output data recorder during consolidation of the specimen #Tae6 by flash spark plasma sintering method. A tantalum foil was placed between powder and graphite foil while the specimen was subjected to preheating stage. This foil was in contact with pre-consolidated specimen during FSPS step and significantly decreased the incubation time for flash sintering.

Fig. 7. Typical fracture surfaces of specimen #Tae6 consolidated by flash SPS after flexural strength tests at 1600 °C. (b, d) show opposite sides of a bar after flexural strength test. (c) shows the magnified area of (b) with a 100 μm nonequiaxial grain of silicon carbide.

Graphical Abstract (for review)

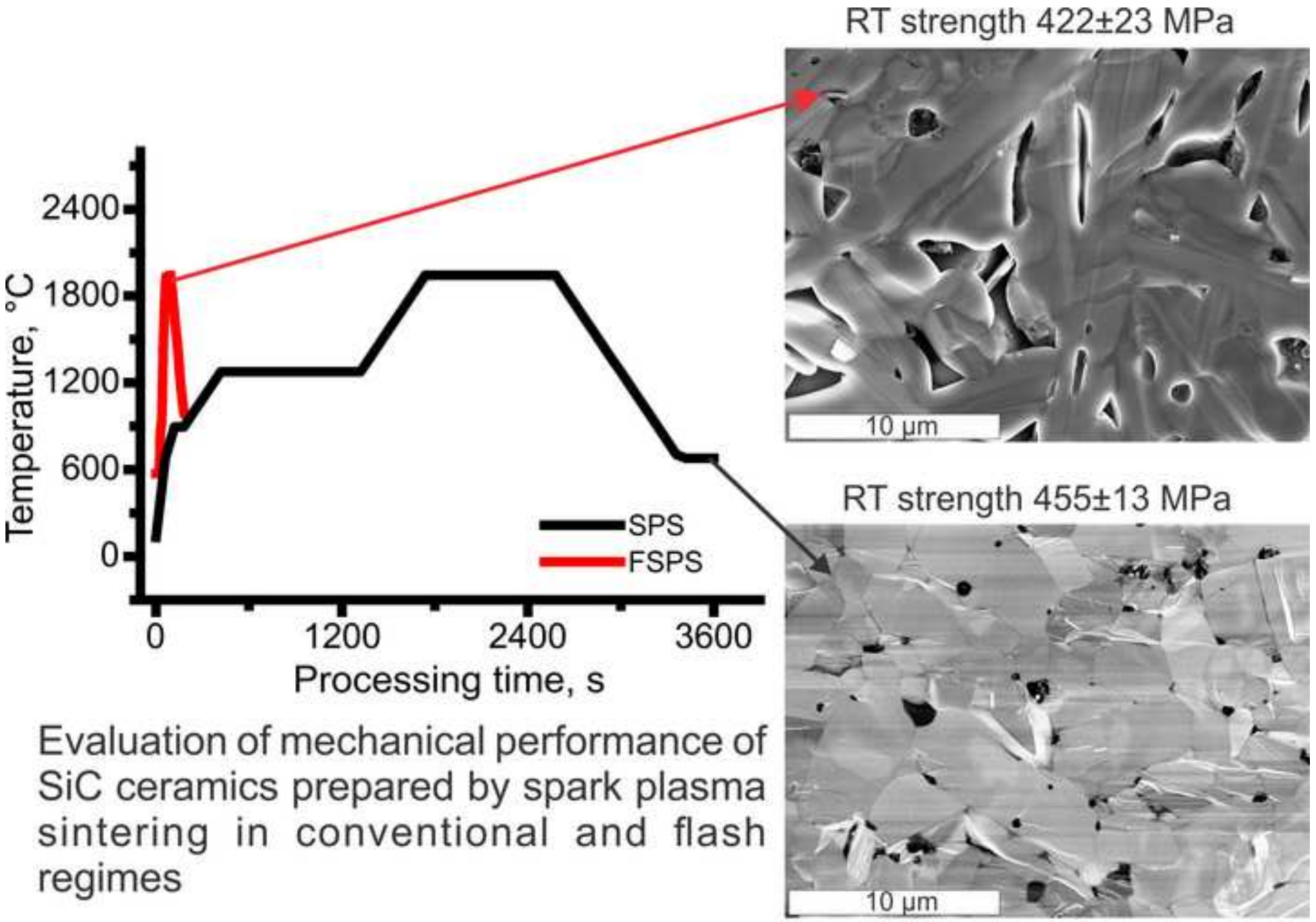

Evaluation of mechanical performance of SiC ceramics prepared by spark plasma sintering in conventional and flash regimes

Hot-spots generation, exaggerated grain growth and mechanical performance of silicon carbide bulks consolidated by flash spark plasma sintering

Highlights

- Mechanical performance of flash consolidated ceramics is reported for the first time.
- SiC specimens with 30 or 50 mm in diameter have been prepared.
- Acceptable level of flexural strength (380–420 MPa) was achieved.
- The optimization routes for flash consolidation of SiC were proposed.

Figure 1
Click here to download high resolution image

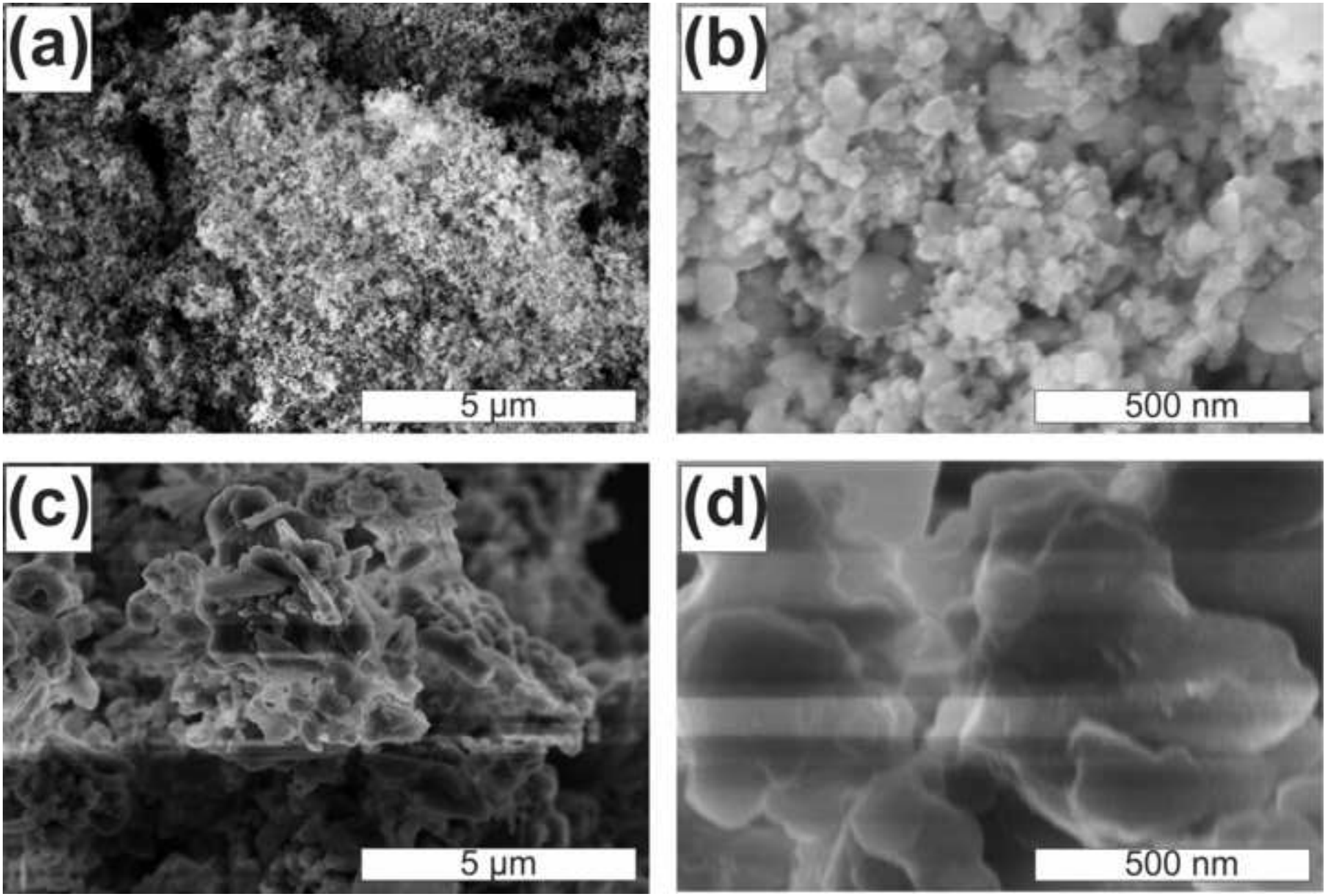

Figure 2

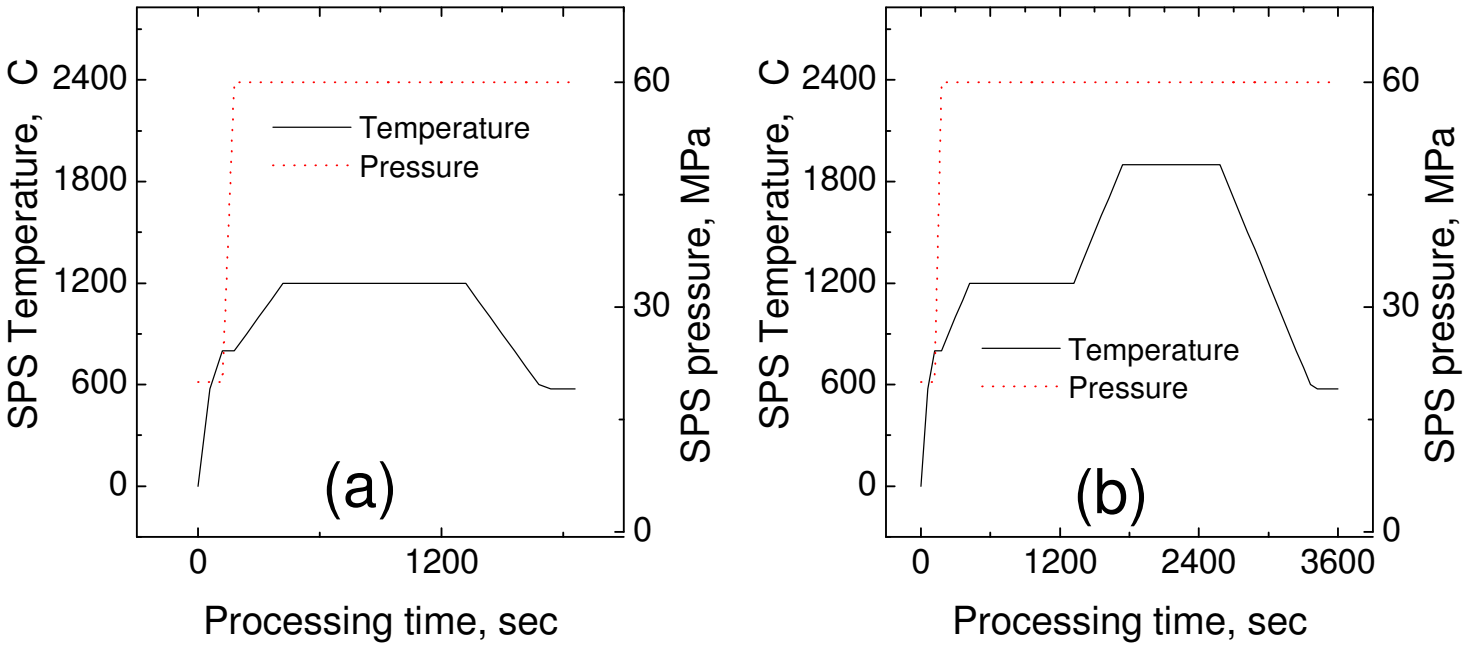
SPS Temperature, C
2400
1800
1200
600
0
60
30
0
SPS pressure, MPa
Temperature
Pressure
(a)
0
1200
Processing time, sec
SPS Temperature, C
2400
1800
1200
600
0
60
30
0
SPS pressure, MPa
Temperature
Pressure
(b)
0
1200
2400
3600
Processing time, sec

Figure 3

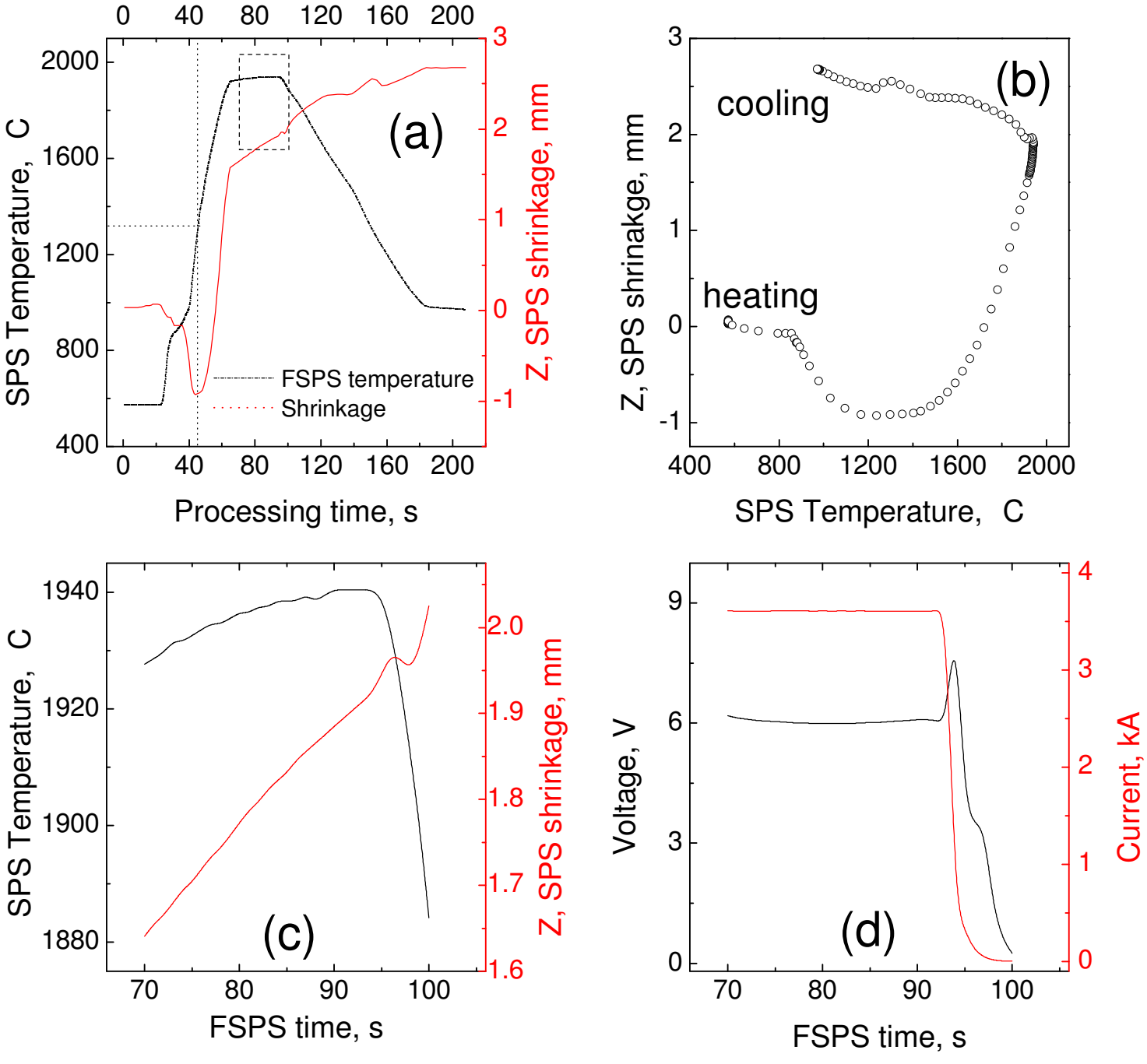
(a)
SPS Temperature, C
Z, SPS shrinkage, mm
Processing time, s
FSPS temperature
Shrinkage
(b)
cooling
heating
Z, SPS shrinakge, mm
SPS Temperature, C
(c)
SPS Temperature, C
Z, SPS shrinkage, mm
FSPS time, s
(d)
Voltage, V
Current, kA
FSPS time, s

Figure 4

Click here to download high resolution image

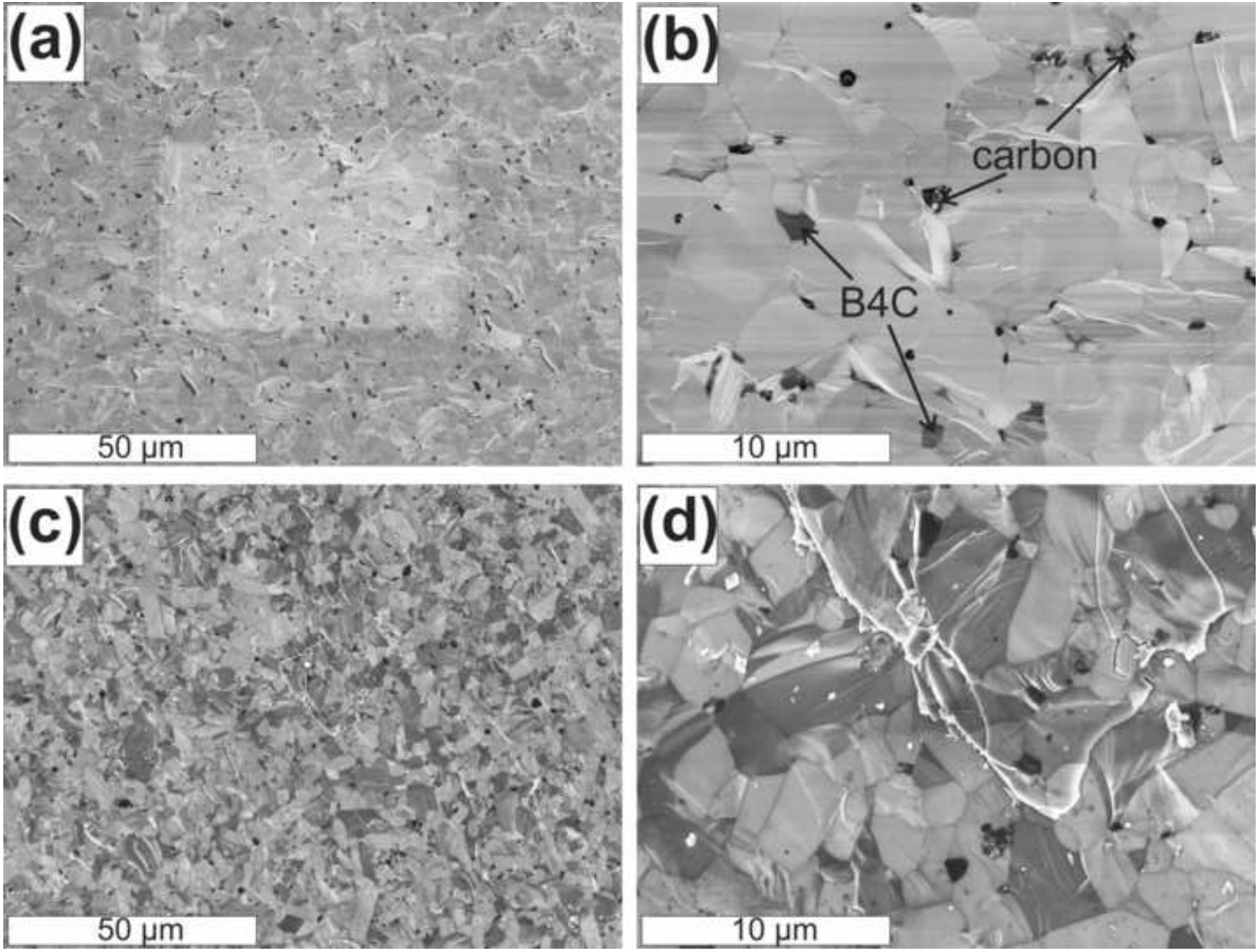

Figure 5

Click here to download high resolution image

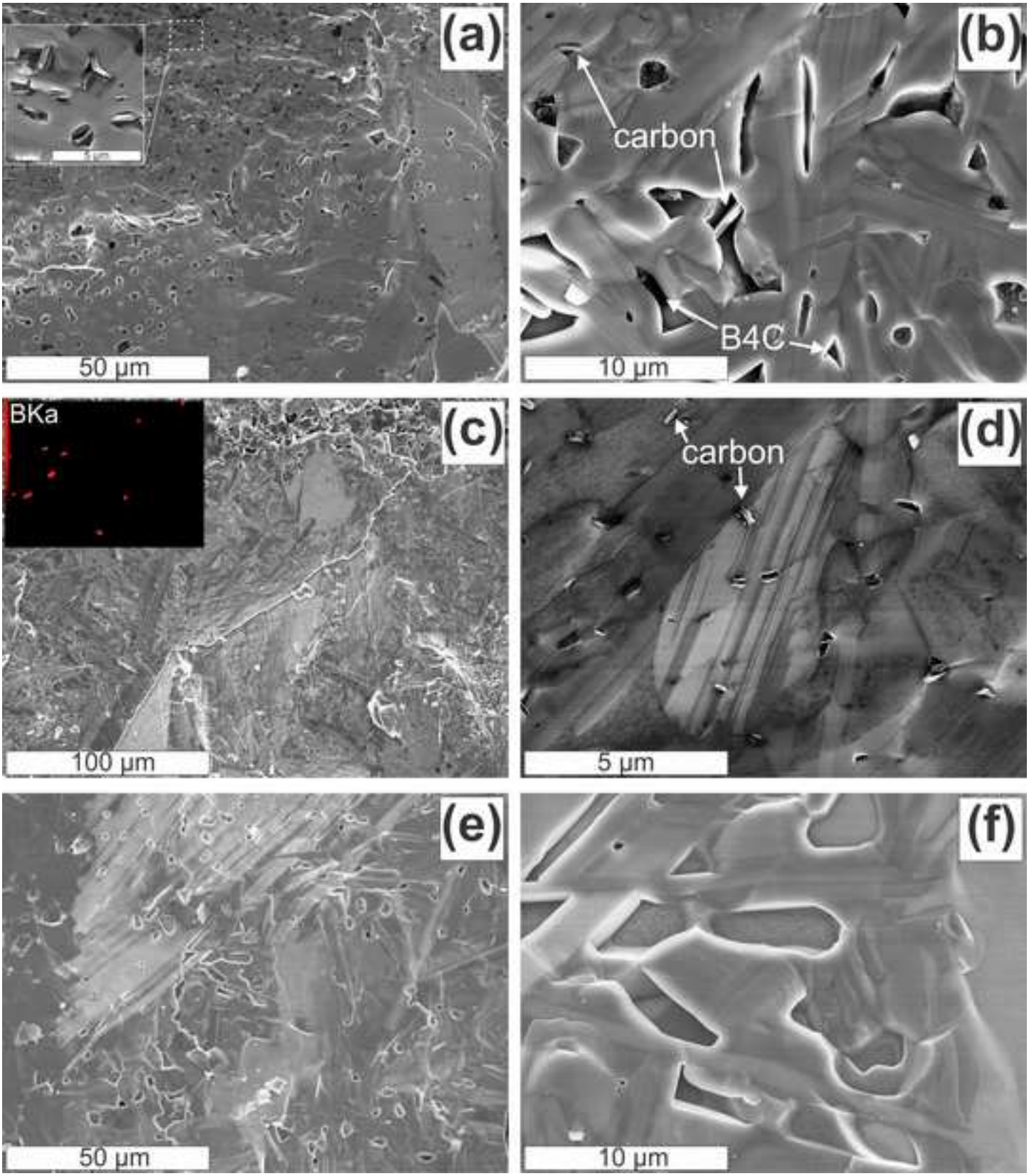

Figure 6

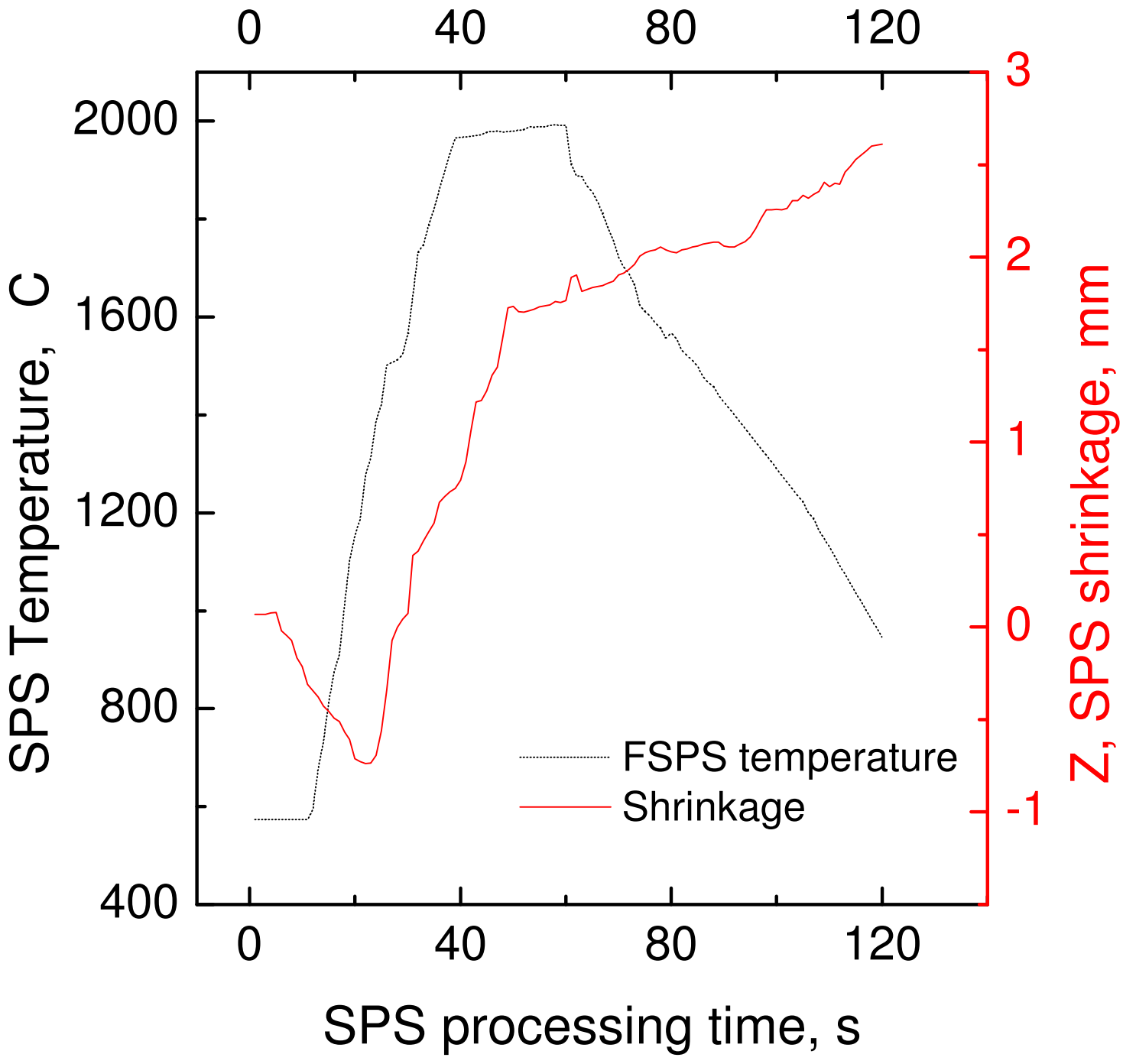
0
40
80
120
2000
1600
1200
800
400
SPS Temperature, C
3
2
1
0
-1
Z, SPS shrinkage, mm
FSPS temperature
Shrinkage
SPS processing time, s

Figure 7

Click here to download high resolution image